Chen, Liwei; Huang, Shilin; Ras, Robin H.A.; Tian, Xuelin

Omniphobic liquid-like surfaces

Published in:
Nature Reviews: Chemistry

DOI:
10.1038/s41570-022-00455-w

Published: 01/02/2023

Document Version
Peer-reviewed accepted author manuscript, also known as Final accepted manuscript or Post-print

Please cite the original version:
Chen, L., Huang, S., Ras, R. H. A., & Tian, X. (2023). Omniphobic liquid-like surfaces. *Nature Reviews: Chemistry*, *7*(2), 123-137. https://doi.org/10.1038/s41570-022-00455-w

Omniphobic liquid-like surfaces

Liwei Chen[1,2], **Shilin Huang**[1,2], **Robin H. A. Ras**[3,4,*], **and Xuelin Tian**[1,2,*]

[1]School of Materials Science and Engineering, Key Laboratory for Polymer Composite & Functional Materials of Ministry of Education, Guangzhou Key Laboratory of Flexible Electronic Materials and Wearable Devices, Sun Yat-sen University, Guangzhou 510006, P. R. China.
[2]State Key Laboratory of Optoelectronic Materials and Technologies, Sun Yat-sen University, Guangzhou 510006, P. R. China.
[3]Department of Applied Physics, Aalto University School of Science, Espoo 02150, Finland.
[4]Center of Excellence in Life-Inspired Hybrid Materials (LIBER), Aalto University, 02150 Espoo, Finland.
[*]e-mail: tianxuelin@mail.sysu.edu.cn; robin.ras@aalto.fi

Abstract

Many of the recent advances in liquid repellency are linked to smooth solid surfaces with covalently grafted flexible polymer brushes or alkyl monolayers. The surface-tethered flexible species are highly mobile at room temperature and endow the solid surfaces with unique liquid-like quality and unprecedented dynamical repellency (i.e., ultralow contact angle hysteresis) towards various liquids, regardless of their surface tension. Omniphobic liquid-like surfaces (LLSs) thus provide a promising alternative to prevalent air-mediated superhydrophobic or superoleophobic surfaces and lubricant-mediated slippery surfaces to address the challenges in minimizing surface-liquid interfacial adhesion, while avoiding fabrication complexity and air/lubricant loss issues of the latter two types of surfaces. More importantly, the liquid-like layer controls many important interface properties, such as slippage, friction, and adhesion, which may bring novel functions and applications that are inaccessible to conventional solid coatings. In this review, we introduce the basic concepts related to LLSs and discuss their inherent dynamic dewetting/omniphobic mechanisms. Particular emphases are given to two aspects: the fundamental principles for surface design and the consequences of the liquid-like nature for task-specific applications. Key challenges and opportunities for omniphobic LLSs are also overviewed.

1. Introduction

Surface wettability or de-wettability is a crucial consideration in many aspects of daily life and industry. Advanced dewetting surfaces with ultralow liquid adhesion have attracted rapidly increasing interest because of their tremendous application potential in many fields that require materials capable of fouling resistance,[1] icephobicity,[2] drag reduction,[3] oil/water separation,[4] or enhanced heat transfer.[5] Inspired by natural biological surfaces and benefitted from progress in nanofabrication techniques, a large number of advanced liquid-repellent surfaces have been developed since the later 1990s,[6-8] such as air-mediated superhydrophobic surfaces (SHPSs) and superoleophobic surfaces (SOPSs),[9,10] and liquid-mediated slippery lubricant-infused porous surfaces (SLIPSs).[11] These surfaces have distinct surface/interface design principles, which determine their advantages as well as limitations in practical application scenarios.

For air-mediated superlyophobic surfaces, roughening hydrophobic materials with hierarchical micro/nanostructures is a universal fabrication strategy for SHPSs,[12] or even SOPSs if reentrant structures are constructed.[13,14] By conceiving an air-like layer beneath the probe droplet (air is trapped in surface microstructures and the droplet settles atop them, forming a solid-air-liquid composite interface), the liquid-solid contact area is greatly reduced and the liquid droplet can bead up with a high static contact angle (SCA, $\theta_0 > 150°$) and readily roll down the surfaces (low rolling angle $\theta_{\mathrm{roll}} < 10°$) (Fig. 1b).[15,16] This air-like layer is reminiscent of the famous Leidenfrost phenomenon observed on hot solid surfaces (liquid droplets drift on a vapor surface, see Fig. 1a).[17,18] However, such an air-like layer is unstable that often suffers from liquid intrusion under high pressure or humid condensation conditions,[19,20] and moreover, fine surface micro/nanostructures are very vulnerable to mechanical damage.[21,22] For liquid-mediated slippery surfaces (i.e., SLIPSs), the design strategy is to displace the unstable air in the microstructures with a suitable liquid. The infused liquid (mostly perfluorinated polymers) is immiscible with the probe droplets and can serve as a slippery liquid lubrication layer to facilitate the sliding of probe droplets on the surfaces (Fig. 1c).[23-25] SLIPSs possess extremely slippery, smooth surface characteristics and negligible contact angle hysteresis (CAH, characterizing the surface pinning effect that resists droplet motion), which make them suitable for repelling whatever immiscible liquids. Nevertheless, such a liquid layer is not durable and may be depleted due to volatilization, migration, and droplet entrainment.[24,25]

Paralleling with the progress of air-mediated surfaces and liquid-mediated surfaces, a new research field is the development of omniphobic liquid-like surfaces (LLSs) by covalently grafting highly flexible polymer brushes or alkyl monolayers onto smooth solid surfaces (Fig. 1d).[26-30] These surface-tethered flexible species are highly mobile and exhibit unique liquid-like nature, for which extremely low CAH can be achieved on the surfaces towards various organic and aqueous liquids, regardless of their surface tensions. The emergence of omniphobic LLSs has substantial implications for interface science. First, excellent liquid repellency is accessible to the smooth solid surfaces based on the liquid-like nature, without relying on surface texturing, thus avoiding complex microstructure manufacturing and structural fragility issues of superlyophobic surfaces. Second, the concerns about interface instability of air- or liquid-mediated liquid-repellent surfaces due to air or lubricant loss cease to exist on such surfaces, since the molecule layer is covalently bonded and not easily washed away or depleted by evaporation. Third, the unique liquid-like characteristic controls many important interface properties, such as slip, friction, and adhesion,[31-35] which may bring novel functionalities that can hardly be realized with conventional solid surfaces. In this review, we discuss the basic concepts related to LLSs and elaborate on their design principles with a focus on the underlying molecular mechanism. We next summarize the preparation methods of LLSs and highlight the emerging applications of LLS-based interface materials. Finally, we address the remaining challenges and give the outlook for future research in this field.

2. Fundamental understanding of liquid-like surfaces

2.1 Wettability, hysteresis and friction on smooth surfaces

As early as 1805, Thomas Young proposed a mechanical model to describe the equilibrium wetting state of a sessile droplet on an ideal solid surface (chemically homogeneous, smooth and rigid) (Fig. 2a).[36] The intrinsic wettability (hydrophobic or hydrophilic) of a smooth solid surface is defined by Young's contact angle (θ_Y)

$$\cos\theta_{\mathrm{Y}} = (\gamma_{\mathrm{sv}} - \gamma_{\mathrm{sl}})/\gamma_{\mathrm{lv}} \qquad (1)$$

where γ_{sv}, γ_{sl}, and γ_{lv} separately denote the solid-vapor, solid-liquid, and liquid-vapor interfacial tensions. Note that an ideal solid surface is assumed in Young's model, which implies that there is only a single thermodynamic stable state (i.e., minimum Gibbs energy) with the contact angle equal to θ_Y.[37-39] However, for a real solid surface, different SCAs can be measured experimentally between unique maximum and minimum angles − the advancing and receding angles (θ_A, θ_R), which corresponds to the critical steady angles for the onset of contact line advancing or receding (Fig. 2b).[27] The difference between θ_A and θ_R is defined as contact angle hysteresis (CAH, $\Delta\theta$)

$$\Delta\theta = \theta_{\mathrm{A}} - \theta_{\mathrm{R}} \qquad (2)$$

which arises from the pinning effects due to the surface structural or chemical heterogeneity.[40,41] The coefficient of static friction (μ_s) at the onset of droplet motion is proportional to the CAH,[42] given by

$$\mu_{\mathrm{s}} = k\Delta\theta/\pi \qquad (3)$$

where k is a shape factor. The static friction force resisting droplet motion is dictated by $F_{\mathrm{f}} = \mu_{\mathrm{s}}F_{\mathrm{N}}$, where $F_{\mathrm{N}} = \pi\gamma_{\mathrm{lv}}w\sin\theta_{\mathrm{Y}}$ is the normal component of the interfacial tension force and w is the droplet contact width. Thereby, the CAH determines whether it is easy to initiate the droplet motion on the surfaces and plays a dominant role in liquid repellency.[30,42-44] For a moving droplet, the coefficient of dynamic friction (μ_d) is proportional to the difference in dynamic advancing and receding contact angles ($\Delta\theta(v) = \theta_A(v) - \theta_R(v)$),[42] given by

$$\mu_{\mathrm{d}} = k\Delta\theta(v)/\pi \qquad (4)$$

which is dependent on the droplet velocity (v). The recognition that low CAH can be different from low dynamic friction is a reminder that designing a surface that can easily initiate droplet motion may not be the same as designing a surface that has rapid droplet shedding.

2.2 Liquid-like concept and omniphobic mechanism

Chemical grafting of polymer brushes and alkyl monolayers is a common strategy for surface (de-)wettability regulation.[45,46] However, in retrospect, most studies on (de-)wettability regulation have focused primarily on the surface energy rather than the dynamics of surface-grafted functional groups. The relationship between chain flexibility and surface dewetting properties was first reported by McCarthy's group for the use of grafted flexible groups to obtain ultralow CAH on smooth solid surfaces.[27,29,30] They attributed their ultralow CAH for both water and organic liquids to the liquid-like nature of surface-grafted flexible species, and thus put forward a novel liquid-repellent system − liquid-like surfaces (LLSs).

The concept of “liquid-like” has been proposed in previous studies on polymer glasses, which found that the molecular chains on the surface are more mobile (many orders of magnitude) than the interior.[47-49] However, it was not associated with surface de-wettability. As is known, there are three physical states for amorphous polymers − glassy state, rubbery state and fluid state, as a result of temperature-dependent chain mobility (Fig. 2c).[50] Similar to the glass-to-fluid transition of a bulk polymer, it is rational to speculate on the existence of a change from solid-like state to liquid-like state for the grafted polymers with different glass transition temperature (T_g) (Fig. 2d). Some highly flexible polymers with extremely low T_g (typically less than -100 °C), such as polydimethylsiloxane (PDMS,

T_g = -127 °C)[51] and perfluoropolyether (PFPE, T_g = -116 °C),[52,53] are liquid and highly mobile at room temperature. Even though one end of the polymer chain is fixed on the surface, the other part is free to rotate, bend and stretch, as is illustrated by an "umbrella model" in Fig. 2e.[29,54] The dynamic chain nature of grafted flexible polymers endows the solid surfaces with unique liquid-like quality at ambient temperature and unprecedented liquid repellency (i.e., ultralow CAH).[27,28,51] Besides highly flexible polymer brushes, the grafted monolayers of branch-structured alkylsilanes could also exhibit liquid-like nature and ultralow CAH for water and organic liquids.[29,30,54]

The liquid-like nature of surface-grafted flexible molecules affects the CAH in two ways. First, LLSs are self-smoothing and chemically homogeneous, because the high mobility of surface-grafted molecular layers enables them to mask the chemical or topographical defects on the solid surfaces,[55] which can reduce the number of metastable states and the energy barriers between them. Second, the grafted molecule chains are rotationally dynamic, which helps to overcome the energy barriers for moving the contact lines of the droplets.[27,29,30] In this sense, the liquid-like molecular layer provides the possibility of bringing a real solid surface close to an ideal surface in terms of minimal CAH.

2.3 Influential factors on liquid-like nature

Considering the effects of the physical nature (solid-like or liquid-like) of surface-grafted molecular layer on CAH, omniphobic LLSs can be designed through the rational regulation of molecular structure and chain properties to achieve high chain mobility. In general, the chain mobility of surface-grafted molecular layer is controlled by many factors, including molecular structure, chain length, grafting density, crosslinking degree, temperature, and solvent effect of probe liquids.

Molecular structure. The molecular structure of backbone chain plays a major role in chain mobility. Related theories of polymer physics have demonstrated that the polymers with repeated Si–O and C–

O bonds have greater chain flexibility than carbon-based polymers with repeated C–C bonds.[56] This can be understood through the structural differences between PDMS, PFPE and polyisobutylene (PIB) in terms of their bond lengths, bond angles, and electronegativities (Fig. 3a, b). First, the Si–O bonds (1.63 Å) and Si–C bonds (1.90 Å) in PDMS are much longer than the C–O bonds (1.44 Å) and C–C bonds (1.58 Å) in PFPE, as well as the C–C bonds (1.53 Å) in PIB.[57-60] Second, the bond angles of PDMS (143° and 112°) and PFPE (120°, 115°, and 111°) are much greater than that of PIB (109.5°).[57-60] The larger bond lengths and angles imply that the constituent atoms of PDMS (Si and O) and PFPE (C and O) are much further apart compared with those of PIB (C and C). The large distances between the constituent atoms create more "free space" for intramolecular rotation. The third factor is their differences in electronegativity between constituent atoms of Si (1.8), O (3.5), C (2.5), and F (4.0).[52,57-60] The large electronegativity difference will endow the bonds with more ionic nature. For example, according to Pauling's electronegativity, the Si–O bonds are more ionic rather than generally considered covalent.[61] The ionic nature adds a great deal of flexibility to the backbones for a low rotation barrier. The rotation energy for Si−O bond (1.9 kJ mol^{-1}) in PDMS is about 1−2 orders of magnitude weaker than that for C−C bond (23.7 kJ mol^{-1}) in PIB, even below the ambient thermal energy threshold ($kT \approx 2.5$ kJ mol^{-1}).[62] These attributes contribute to the high chain flexibility and low T_g values of PDMS and PFPE that are unavailable to carbon-based polymers. Recent studies have identified that linear PDMS, PFPE, and their derivatives, such as polymethylhydrosiloxane (PMHS, T_g = -140 °C),[63] are ideal flexible polymers for designing omniphobic LLSs to achieve ultralow CAH ($\Delta\theta < 5°$).[51,52,64] Note that crosslinking between molecular chains can restrict chain mobility and endow the materials with a solid-like nature (Fig. 3g). This is why cross-linked PDMS coatings have much higher CAH than the surface-grafted linear PDMS monolayers.[64] The poor chain mobility of the cross-linked polymer coatings can be remedied by using a non-stoichiometric composition ratio or reintroducing pendent flexible chains, thereby restoring low CAH on the surfaces.[65-67]

Grafting density. Packing or grafting density is another important factor influencing the mobility of surface-grafted polymer chains. A general definition of grafting density is determined by $\sigma = (h\rho N_{\mathrm{A}})/M_{\mathrm{n}}$, where h is polymer layer thickness, ρ is polymer density, and N_{A} is Avogadro's number, and M_{n} is molecular weight of the polymer.[64,68] Here, σ means the number of chains per unit area. However, it cannot reflect the packing characteristics (overlapping or non-overlapping) of the surface-grafted chains. A more indicative parameter is the dimensionless grafting density $\Sigma = \sigma\pi R_{\mathrm{g}}^2$, where R_{g} is the radius of gyration of the polymer chain.[64,68] The physical interpretation of Σ is the number of chains that occupy an area that a free non-overlapping polymer chain would normally fill under the same experimental conditions. Therefore, the dimensionless parameter Σ is reliable for judging the chain conformation in a grafted polymer layer. Previous research has identified three regimes in molecular chain conformation (Fig. 3c): the "mushroom" regime at $\Sigma < 1$ (Regime I), the "mushroom-to-brush" transition regime at $1 < \Sigma < 5$ (Regime II), and the highly stretched "brush" regime at $\Sigma > 5$ (Regime III).[68] When $\Sigma < 1$, the grafted chains are separated far and the underlying solid substrate will be exposed to the probe liquids. When $\Sigma > 5$, the grafted chains are closely packed in a highly stretched brush regime and behave rigidly. The desirable condition for designing LLSs is $\Sigma = 1{-}2$, under which the grafted chains are moderately packed and able to rotate freely.[51,64]

The effects of grafting density on chain mobility and droplet motion is particularly obvious for self-assembled organosilane monolayers. The monolayers with relatively loosely packed alkyl chains can exhibit liquid-like nature and remarkably low CAH.[69] However, most self-assembled alkylsilane monolayers reported in literature often have very high grafting density. The closely packed alkylsilane layers can be described as solid-like, similar to a layer of bulk alkane solid in nature, which usually exhibit sizable CAH.[70] To obtain low CAH on the alkylsilane monolayers, three strategies are suggested to reduce the grafting density (Fig. 3d). The first strategy is using branch-structured alkylsilanes (Route A).[29,30,54] The second strategy is introducing molecular spacers between the neighboring alkyl chains (Route B).[71-73] The third strategy is shortening the reaction time (Route C).[69]

Chain length. Chain length or molecular weight (MW) is also important for the chain mobility of grafted layer. In a typical case, the CAH for water and organic liquids on the PDMS-grafted surfaces are observed to be MW-dependent.[59,64,74] As shown in Fig. 3e, f, when the MW of PDMS increases from 10^2 to 10^5 g mol^{-1}, the thickness of grafted PDMS layer increases, and the grafting density decreases monotonically. However, the CAH values decrease first (MW < 10^3 g mol^{-1}) and then increase (MW > 10^4 g mol^{-1}) for both water and organic liquids with increasing PDMS MW. In other words, both too low and too high PDMS MW are not conducive to obtaining low CAH on the surface. When the PDMS MW is too low (MW < 10^3 g mol^{-1}), the grafted layer is so thin that the residual silanols on the surface are exposed, resulting in droplet pinning. When the MW is too high (MW > 10^4 g mol^{-1}), there are two explanations to understand the resulting high CAH. The first explanation concerns the spontaneous spreading of grafted PDMS chains at the three-phase contact line onto the liquid droplet surface.[75] When the contact line moves, the spreading and retracting of PDMS chains have to occur reversibly. The high-MW chains will spread further from the contact line onto the droplet surface, and their sluggish spreading/retracting kinetics impedes the contact line motion. Another explanation is that the grafted polymer layer distorts at the three-phase contact line to respond to the shearing force from the moving contact line. When the MW is high, the polymer layer is thick and viscous, and the surface-liquid interface distorts at the contact line to form a “lens”, which contributes to the CAH.[59,64] Empirically, the ideal MW interval for PDMS to obtain the minimum CAH on the surface is between 2×10^3 and 1×10^4 g mol^{-1} (Fig. 3f).[27,51,55,59,64,74]

Solvent effect and temperature. Besides the above internal factors, some external factors, such as solvent effects of probe liquids and substrate temperature, also have great influence on the chain mobility of surface-grafted layer. An unusual phenomenon on the LLSs is that organic liquids have lower CAH values than water even though they have much lower SCA values.[51,64] These organic liquids are usually good solvents for the polymer. It is speculated that this unusual phenomenon might originate from the affinity between the probe liquids and the grafted layer. When the surface-grafted polymers contact with a poor solvent (i.e., water), the solvent molecules are unlikely to enter the chains and the grafted polymers tend to form a collapsed chain conformation, described by a "discrete liquid-liquid interface" (Fig. 3h).[28,51] However, when the surface-grafted polymers contact with a good solvent, the solvent molecules most likely enter the chains and swell the polymer brush layer, described by a "blended liquid-liquid interface" (Fig. 3i).[28,51] The swelling state by organic liquids benefits the suppression of terminal relaxation time and the enhancement of chain mobility,[51] which should be responsible for their lower CAH for organic liquids. In addition, moderately elevated temperature could also promote the mobility of grafted chains on the surface.[51,52] For liquid polymers (e.g., PDMS, PFPE), their viscosity decreases with temperature and surface-grafted polymer chains become more mobile as temperature increases, resulting in a further decrease in CAH.[76] This manifests in the thermal-responsive liquid repellency of LLSs.

3. Fabrication of liquid-like surfaces/coatings

3.1 Liquid-like monolayers

According to the type of surface-grafted molecules, LLSs can be classified into hydrophobic PDMS-, PFPE-, alkyl-grafted surfaces, and hydrophilic polyethylene glycol (PEG)-grafted surfaces (Fig. 4a).

PDMS-grafted LLSs. The surface-grafted PDMS brushes, also known as "covalently attached liquid",[77] can be prepared through either the grafting-to or grafting-from route. The grafting-to route involves the chemical reaction of preformed linear PDMS with a surface. Two typical grafting-to strategies are: 1) PDMS is grafted to inorganic oxide surfaces by heat treatment (typically above 100 °C),[27,55,59] or UV light irradiation.[78,79] The reaction mechanism is that the activated hydroxyl groups and water molecules on inorganic oxide surfaces partially cleave Si–O–Si bonds of surrounding PDMS, and these segmented PDMS chains form covalent Me–O–Si (Me: Metal) bonds with the surfaces. Butt *et al*. reported that PDMS could be grafted to inorganic oxide surfaces at room temperature, though the grafting process is slow.[80] These methods are universal to silicones, even PDMS with inactive trimethylsilyl-termination. 2) PDMS is grafted to a surface by using end-functionalized PDMS (e.g. hydrogen-, vinyl-, epoxy-, amino- and thiol-terminated PDMS).[81,82] This method requires the surface to have complementary functional groups. For example, the vinyl-terminated PDMS covalently binds with the Si–H functionalized surfaces in the presence of Pt catalysts.[64]

The grafting-from route involves the polycondensation of reactive monomers on a surface. Representative grafting-from strategies to create PDMS brushes include: 1) PDMS is grown from solution by polycondensation of monomers. There are two commonly used reactive monomers, namely dimethyldimethoxysilane (DMDMOS) and dimethyldichlorosilane (DMDCS).[77,83] Through the acid-catalyzed polycondensation of DMDMOS in solution, a smooth PDMS layer on a hydroxylated surface is formed within a few minutes.[77] For active DMDCS, reactive growth of PDMS happens spontaneously through the polymerization of DMDCS under hydrolysis of Si–Cl groups without catalysts.[83] 2) PDMS is grown through vapour phase deposition of chlorine-terminated siloxanes.[84-86] This is a solvent-free grafting-from method in which the reactive growth and covalent grafting of PDMS could rapidly proceed in the presence of moisture via polycondensation of hydrolyzed silanols on the hydroxylated surfaces.

PFPE-grafted LLSs. Linear PFPE is a kind of fluorinated flexible polymer with extremely low T_g and high chain mobility comparable to linear PDMS. Compared with PDMS, PFPE has a lower surface energy so that PFPE-grafted LLSs have larger contact angles for water and organic liquids (Fig. 4b, c). A typical strategy to prepare PFPE-grafted LLSs is utilizing the diluted trimethoxysilyl-terminated PFPE to react with hydroxyl-activated substrates through a simple dip-coating process followed by heat treatment at 100−150 °C.[52,87,88]

Alkyl-grafted LLSs. It has been known that densely grafted alkyl chains are crowded, less mobile, and behave as a rigid (solid-like) surface to probe liquids.[69,70] To enable the alkyl chains to rotate freely and project the liquid-like nature, the methods of introducing molecular spacers and controlling reaction time has been proposed to control the grafting density.[69,71-73] In addition, McCarthy's and Hozumi's groups found that the monolayers of branch-structured alkylsilanes, such as tris(trimethylsiloxy)silylethyldimethylchlorosilane and bis((tridecafluoro-1,1,2,2,-tetrahydrooctyl)-dimethylsiloxy)methylsilane, could exhibit ultralow CAH.[29,30,54]

PEG-grafted LLSs. Different from PDMS-, PFPE- and alkyl-grafted surfaces which are statically oleophilic/hydrophobic ($\theta_{\mathrm{oil}} < 90°$, $\theta_{\mathrm{water}} > 90°$) but dynamically oleophobic/hydrophobic ($\Delta\theta_{\mathrm{oil}}$ and $\Delta\theta_{\mathrm{water}} < 10°$), PEG-grafted LLSs exhibit a paradoxical property of static hydrophilicity but dynamical hydrophobicity ($\theta_{\mathrm{water}} < 90°$, $\Delta\theta_{\mathrm{water}} < 10°$) (Fig. 4b,c).[89] It should be attributed to the high surface energy and flexible C−O bonds of PEG chains, which endow the PEG-grafted surfaces with both hydrophilic property and liquid-like nature, so that water droplet slides easily on such hydrophilic surfaces. Hydrophilic PEG-grafted LLSs can be prepared by using PEG-ylated organosilane, such as 2-(methoxypoly(ethyleneoxy)$_x$-propyl)-trimethoxysilane, to react with hydroxylated solid surfaces.[90,91]

3.2 Durable liquid-like coatings

Early studies in preparing omniphobic LLSs focused on the chemical grafting of a molecularly thin monolayer of flexible polymers or alkyl groups onto solid surfaces. However, such monolayers with a thickness of only a few nanometres have poor mechanical durability in practical applications. To this end, an enormous research effort has been devoted to develop durable liquid-like coatings.[92-95]

Surface deterioration usually results from either physical damage or chemical decomposition. To cope with physical damages (e.g., wear, scratch), three main strategies are suggested (Fig. 4d). The first strategy is to create a thick coating with a self-similar composition/structure to increase its wear tolerance.[96] The liquid-like polymers are uniformly interspersed in the entire coating and thus the removal of a top layer will expose the embedded functional moieties (route i in Fig. 4d). As such, the coatings can retain their dynamic omniphobic properties as long as there are still some coating materials left on the solid surface. Liu's group developed a series of durable omniphobic coatings based on PFPE- or PDMS-incorporated polyurethane (PU) via a graft-copolymer-based approach.[97-101] Wearing off the surface layers exposes the PDMS or PFPE nano-reservoirs embedded within the coating matrix and the newly exposed chains regenerate the coating surface.[100,101] Evidently, this is a sacrificial strategy that surface durability relies on the coating thickness and self-similar composition. Even for the thick self-similar composition coatings, their surface omniphobicity is still observed to deteriorate due to increased surface roughness by surface wear. The second strategy is to endow the coatings with structural healing ability (route ii) based on molecular chain migration and chemical bond reconstruction to repair the open defects at room temperature and maintain their liquid repellency after scratching, cutting, and indenting.[102,103] The third strategy is to reinforce the coating hardness and toughness to resist wear (route iii). The key criteria for hard flexible coatings include high hardness (H), high hardness-to-Young's modulus ratio $H/E > 10\%$, and high elastic recovery $w_e > 60\%$.[104] Natural materials with high hardness and toughness are mostly inorganic-organic (I-O) nanocomposites, such as nacre and human teeth, made of proteins and minerals.[105] Recent work demonstrated that the crosslinked oligomeric silsesquioxanes consisting of flexible groups and a ladder-like or cage-like core could meet the above criteria for preparing the wear-resistant hard flexible coatings (Fig. 4e,f).[106-111] Liu's group developed such a durable liquid-like coating with glass-like wear resistance and polymer-like bendability via the photo-initiated polymerization of PDMS-grafted cage-like polyhedral oligomeric silsesquioxane (GPOSS-*g*-PDMS) (Fig. 4e).[110] This coating has a 3.5 times greater H value ($H = 0.7$ GPa), a 5 times higher H/E value ($H/E = 21\%$) and a 2.8 times higher w_e value ($w_e = 79\%$) than that of the PU coatings. Recently, the record hardness for hard flexible liquid-like coatings has been pushed to 1.4 GPa by a copolymer coating of ladder-like polysilsesquioxane bearing PFPE chains (LASQ-*g*-PFPE) (Fig. 4f).[112] The wear resistance of such coatings was much improved and they could resist even after 200 cycles of bending to a curvature radius of 2 mm without cracking and 300 times abrasion with steel wool at a pressure of 26 kPa without loss of omniphobic properties.

Another aspect that should be considered is chemical decomposition caused by gas etching, UV irradiation or high temperature. Gas etching, such as plasma treatment, will decompose the functional segments on the coating surface and produces a high-surface-energy surface. An effective coping strategy is to introduce chemical self-healing ability that the low-surface-energy flexible segments embedded in the coating matrix can spontaneously migrate to the interface and replenish the surface.[96,102] Dealing with ultraviolet and thermal degradation requires chemically stable molecules with high bond dissociation energy, such as silicones and perfluorinated compounds.[52,59] Methyltriethoxysilane-grafted surface could retain omniphobic properties under the high-temperature condition of 350 °C.[113] Recently, Men *et al*. reported a durable organic coating material of highly self-cross-linking methyl etherified melamine formaldehyde resin with PDMS side chains, which could exhibit excellent omniphobicity even after six months of outdoor exposure and 260 h of UV light irradiation.[114]

4. Applications of LLSs and LLS-based interface materials

4.1 Smooth LLSs for anti-liquid/bio/solid-adhesion

Surfaces that passively remove various water- and oil-borne contaminants can help keep clean the world around us, not only for esthetical reasons but also for maintaining functionalities.[115,116] Omniphobic LLSs can readily slide the liquid contaminants for passive removal due to their low CAH (Fig. 5a). It has been reported that the state-of-the-art LLSs (e.g., PDMS-grafted surfaces) could highly repel various liquids regardless of their surface tensions, even for the highly wetting perfluorinated liquids, such as Krytox-101 ($\gamma = 17.0\ \mathrm{mN \cdot m^{-1}}$) and FC-72 ($\gamma = 10.0\ \mathrm{mN \cdot m^{-1}}$),[84,117] and complex fluids, such as urine, crude oil, paints, blood, and various liquid foods.[84,95,118-121] Furthermore, omniphobic LLSs show great potential in anti-fingerprint applications (Fig. 5b).[72,95,101,122,123]

Anti-biofouling and anti-bioadhesion are highly desired surface properties for biomedical materials, and LLSs offer a new anti-bioadhesion strategy. Some recent researches have showed that the PDMS-grafted LLSs had persistent anti-bioadhesion effects to small biomolecules, proteins, cells, and bacteria, even superior to the typical anti-bioadhesion PEG-grafted surface, cross-linked PDMS and slippery SLIPSs (Fig. 5c).[124,125] Their superior anti-biofouling performances should be attributed to the slippery liquid-liquid interface and dynamic nature of PDMS brushes that prevent these biological contaminations from attaching to the surfaces. A series of anti-biofouling applications in medical devices has been demonstrated. For example, the liquid-like PDMS brush could be employed to functionalize the electrodes in biosensors for reducing electrode contamination and noise in complex biofluids,[126] or to modify the intraocular lens for posterior capsular opacification prevention.[127] Moreover, the liquid-like nature of PDMS brushes can be combined with the photocatalytic materials for enhanced anti-biofouling performances.[78,79]

Preventing the aggregation of solid matter, such as ice, scale and wax, on surfaces is important in practice. Recent studies show that the smooth LLSs can serve as sustainable icephobic surfaces to reduce the ice adhesion strength or even passively remove ice because of the slippery ice-liquid interface.[84,128-130] It is noteworthy that the shear ice adhesion measured on the smooth LLSs is shear-rate-dependent.[131] The ice shear strength on the PDMS-grafted surface is reported to as low as 14 kPa at a probe speed of 0.5 mm s^{-1}.[132] When the ice is allowed to detach slowly by self-weight, it could yield an ice adhesion strength of 0.3 kPa, 1000 times lower than a perfluorinated low-surface-energy monolayer (Fig. 5d).[131] Furthermore, Tuteja *et al.* found that the mobile interface of the capped bidentate PDMS-grafted surfaces could dramatically reduce adhesion to various types of solids, including ice (hydrogen bonding), paraffin wax (van der Waals interactions), calcined gypsum (polar bonding), and cyanoacrylate adhesives (covalent bonding).[133] Their anti-solid-adhesion properties regardless of bonding types are attributed to the interfacial slippage.[134]

Surface scaling in desalination, hydroelectric power, and marine transport can lead to reduced heat transfer, increased corrosion, and blockage of pipes or valves. According to classical nucleation theories, it is generally believed that anti-scaling surfaces should be smooth and have low surface energy, so as to reduce the heterogeneous nucleation of scale.[135] However, our group and other researchers recently found that the PDMS brush coatings could exhibit excellent anti-scaling capability, even better than the low-surface-energy fluorocarbon coatings (Fig. 5e).[133,136-138] The superior anti-scaling performances of the PDMS brush coating result from its dynamic, self-smoothing and slippery interface features, which significantly reduces the affinity of salt with the surfaces and inhibit the heterogeneous nucleation of scale. This finding holds great promise for using liquid-like PDMS coatings as a green economical solution to replace environmentally harmful fluorinated coatings to address the scaling problem.

4.2 Patterned LLSs for lossless droplet transport

Directional and spontaneous liquid transport induced by structural anisotropy or surface energy gradient has important applications in many fields, such as bioanalysis, heat transfer and water collection.[139-141] However, conventional liquid-transport surfaces have often encountered problems of liquid transport loss (generally manifested as hardly observable microdroplet residue), which limit their applications.[142] This annoying problem can be addressed by combining LLSs with anisotropic structures or surface energy gradients to realize clean and sustainable liquid transport (Fig. 6a).[87,88,143]

To explore the formation mechanism of microdroplet residues and develop effective inhibition strategies, our group prepared two liquid self-transport surfaces by separately introducing solid 1*H*,1*H*,2*H*,2*H*-perfluorooctyltrichlorosilane (PFOS) coating and liquid-like PFPE coating onto anisotropic surfaces made of radially-arrayed reentrant microstripes (Fig. 6b).[87] We discovered that the formation of microscopic liquid residues is not associated with the CAH but the dynamic receding contact angle ($\theta_{R,d}$). When the velocity of the droplet movement exceeds a certain critical value ($v >$

v_{crit}), the local $\theta_{R,d}$ disappears (i.e., $\theta_{R,d} \rightarrow 0$), and a thin entrained liquid film is generated at the receding end of the sliding droplet. Due to Rayleigh instability, the liquid film ruptures and forms microscopic residues, resulting in lossy liquid transport. Only when $v < v_{crit}$, $\theta_{R,d} > 0$, the entrained-liquid film can be avoided, thus eliminating the microscopic residue (Fig. 6c). The criterion of lossless liquid transport is established according to the Cox-Voinov relation, $\theta_{R,d}^3 = \theta_{R,0}^3 - ACa$, where $Ca = \eta v/\gamma$ is determined by the liquid viscosity (η), the moving velocity (v) and the surface tension (γ) of the liquid, and $A = 9\ln(CY/Y_w)$ is decided by the capillary length (Y) of the liquid (≈ 1 mm), slip length (Y_w) and nonuniversal numerical constant (C). Only below a critical transport velocity when $Ca/\theta_{R,0}^3$ is less than $1/A$, the microscopic liquid residues can be eliminated.[87] Compared with the solid PFOS coating, liquid-like PFPE coating has a larger intrinsic receding angle ($\theta_{R,0}$) and larger slip length (Y_w), thus allowing a larger critical velocity for the occurrence of microscopic residue. As such, the liquid-like PFPE layer provides an effective strategy to inhibit the formation of micro-liquid residues and realize completely lossless droplet transport even at greatly enhanced transport velocity.[87,144]

LLSs have also been deployed to construct anisotropic surface chemistry for lossless droplet self-transport. Dai's group prepared a PDMS-grafted LLS with gradient grafting density by a vapor diffusion-controlled process and realized lossless self-propulsion of droplets with surface tensions down to 10.0 $\text{mN}\cdot\text{m}^{-1}$.[117] Soltani and Golovin designed a wettability-patterned surface with wedge-shaped PDMS channels that are surrounded by a PFPE background.[88] The areas of PDMS and PFPE have different surface energies of 21.8 and 15.2 $\text{mJ}\cdot\text{m}^{-2}$ and similarly low CAH of below 2°. Such surfaces could achieve lossless and long-range (over 150 mm) self-transport of low-surface-tension liquids.

4.3 LLS-based porous materials for liquid separation

Porous membranes and sponges are the main materials for liquid separation. However, serious fouling problems and low separation speed restrict their wide applications in practice, such as crude oil spill remediation. The integration of liquid-like nature and porous materials is expected to design new material systems to deal with pore fouling problems.[145,146] Our group proposed a grafted-liquid lubrication strategy by covalently grafting liquid-like PDMS brushes onto the stainless steel mesh (SSM) membranes to prepare LLS-based membrane materials (LPDMS-SSM) (Fig. 6d).[147] Three membranes with solid coatings of cross-linked PDMS (CPDMS), octadecyltrichlorosilane (OTS), and PFOS were prepared as comparison samples. Because of the slippery and low-adhesion characteristics, the liquid-like PDMS brush layer is expected to reduce the foulant adhesion and promote liquid transport inside the membrane pores (Fig. 6e). Indeed, the viscous crude oil/water separation results showed that the LPDMS-SSM membrane could maintain at least a twice higher average oil permeation flux than the other three solid membranes, and its advantage was more significant in the terminal period (Fig. 6f). The LPDMS-SSM membrane also exhibited impressive antifouling ability that a crude oil film could spontaneously retract and completely detached from the membrane surface. Though SSMs with micron-scale pores were used in our exploratory research, this grafted-liquid lubrication strategy can be applied to the membranes with nano-scale pores to achieve more pronounced performances as the interface lubrication effect is expected to be more prominent for nanopores with high specific surface areas. We further introduced this strategy into three-dimensional (3D) porous sponges to prepare LLS-based oil sorbents.[148] The PDMS brushes act as a covalently-grafted lubrication layer throughout the 3D network channels of the sponge, which can minimize CAH and reduce friction between the oil and sponge channel. Compared to the sponge coated with prevalent cross-linked PDMS, the linear PDMS-grafted melamine sponge exhibited significantly enhanced absorption speed and superior desorption dynamics towards viscous crude oils. Additionally, because of the excellent anti-scaling ability of LLSs, this grafted-liquid lubrication strategy has been applied to distillation membranes to resist scale deposition.[149,150] The design strategy of grafted-liquid lubrication opens a new avenue for developing advanced LLS-based porous materials to achieve superior anti-fouling ability and improved separation performances.

5. Conclusions and outlook

LLSs represent a type of emerging interface materials with macroscopic surface properties controlled by molecular-level chain flexibility. Insights into the surface structure-property relationship identify that ultralow-CAH omniphobic LLSs can be designed by grafting the low-T_g flexible polymers (e.g., PDMS, PFPE) with appropriate molecular weight, or the alkylsilanes with branched structures or loose packing density. The omniphobic LLSs have advantages over conventional liquid-repellent surfaces in terms of ease of preparation, interface stability, and shape retention when used as functional coatings. Their unique interface properties hold great promise in developing innovative materials with unprecedented functionalities that can hardly be realized with conventional solid interface engineering.

Despite remarkable development of the omniphobic LLSs, key challenges remain in this filed. First of all, current knowledge on the LLS-liquid interface configuration and the microscopic wetting process is preliminary and largely based on hypothesis. Endeavors are required to develop molecular-level experimental and theoretical methods to verify how chain flexibility and other properties influence the interface configuration and liquid wetting kinetics on LLSs. Regarding practical applications, limited mechanical and chemical stability of LLSs pose another challenge. Although some durable liquid-like coatings have been reported, solvent-free and easily curable coating formulations capable of constructing environmental-benign durable LLSs with uncompromised omniphobicity are still lacking. In addition, while LLSs offer very low CAH, the relatively slow droplet sliding on them indicates that LLSs can only serve as low-pinning, low-velocity shedding surfaces. If the droplet velocity is extremely low, the liquid may evaporate before sliding off, which might hinder their applications in certain scenarios.

In future work, interface engineering based on highly flexible molecules will continue to push the development of omniphobic LLSs towards functionalization and real-world applications (Fig. 7). Four aspects ranging from chemistry, interface, materials to applications need to be further explored. i) Chemistry: Synthesis of new-type flexible polymers with tunable flexibility and surface energy, enhanced chemical/mechanical durability and self-healing ability is necessary for the on-demand design of LLSs. ii) Interface: Monitoring the kinetics and quantitatively evaluating the mobility of surface-grafted molecular chains, especially when exposed to liquids, is challenging but necessary. In-situ and real-time observation of the evolution of LLS-liquid interface configuration is important for understanding the microscopic repellency mechanism of LLSs towards various liquids. The development of computational models could help clarify the physical states of molecular chains in contact with probe liquids and the underlying dewetting mechanism at the molecular level. iii) Materials: Apart from two-dimensional (2D) flat surfaces, other-dimensional materials can be integrated with the liquid-like nature for new opportunities. For example, the liquid-like layer can be used to modify nanoparticles (0D), nanotubes or nanowires (1D), porous membranes (2D) and sponge (3D) to develop novel material systems. Some researchers have described a family of functionalized nanomaterials that exhibit liquid-like fluidity in the absence of any solvent, such as PDMS-functionalized carbon nanotubes.[151] iv) Applications: Based on the slippery interface and dynamic chain characteristics of omniphobic LLSs, more possibilities of interdisciplinary research need to be explored to achieve new functions and applications in the fields of environment, biology and energy.

References

1 Dhyani, A. *et al.* Design and applications of surfaces that control the accretion of matter. *Science* **373**, eaba5010 (2021).

2 Kreder, M. J., Alvarenga, J., Kim, P. & Aizenberg, J. Design of anti-icing surfaces: smooth, textured or slippery? *Nat. Rev. Mater.* **1**, 1-15 (2016).

3 Lee, C. & Kim, C.-J. Underwater restoration and retention of gases on superhydrophobic surfaces for drag reduction. *Phys. Rev. Lett.* **106**, 014502 (2011).

4 Chu, Z., Feng, Y. & Seeger, S. Oil/water separation with selective superantiwetting/superwetting surface materials. *Angew. Chem. Int. Ed.* **54**, 2328-2338 (2015).

5 Wen, R., Xu, S., Ma, X., Lee, Y.-C. & Yang, R. Three-dimensional superhydrophobic nanowire networks for enhancing condensation heat transfer. *Joule* **2**, 269-279 (2018).

6 Liu, M., Wang, S. & Jiang, L. Nature-inspired superwettability systems. *Nat. Rev. Mater.* **2**, 1-17 (2017).

7 Su, B., Tian, Y. & Jiang, L. Bioinspired interfaces with superwettability: from materials to chemistry. *J. Am. Chem. Soc.* **138**, 1727-1748 (2016).

8 Wang, S., Liu, K., Yao, X. & Jiang, L. Bioinspired surfaces with superwettability: new insight on theory, design, and applications. *Chem. Rev.* **115**, 8230-8293 (2015).

9 Deng, X., Mammen, L., Butt, H.-J. & Vollmer, D. Candle soot as a template for a transparent robust superamphiphobic coating. *Science* **335**, 67-70 (2012).

10 Yong, J., Chen, F., Yang, Q., Huo, J. & Hou, X. Superoleophobic surfaces. *Chem. Soc. Rev.* **46**, 4168-4217 (2017).

11 Wong, T.-S. *et al.* Bioinspired self-repairing slippery surfaces with pressure-stable omniphobicity. *Nature* **477**, 443-447 (2011).

12 Li, X.-M., Reinhoudt, D. & Crego-Calama, M. What do we need for a superhydrophobic surface? A review on the recent progress in the preparation of superhydrophobic surfaces. *Chem. Soc. Rev.* **36**, 1350-1368 (2007).

13 Tuteja, A. *et al.* Designing superoleophobic surfaces. *Science* **318**, 1618-1622 (2007).

14 Liu, T. & Kim, C.-J. Turning a surface superrepellent even to completely wetting liquids. *Science* **346**, 1096-1100 (2014).

15 Lafuma, A. & Quéré, D. Superhydrophobic states. *Nat. Mater.* **2**, 457-460 (2003).

16 Wang, S. & Jiang, L. Definition of superhydrophobic states. *Adv. Mater.* **19**, 3423-3424 (2007).

17 Vakarelski, I. U., Patankar, N. A., Marston, J. O., Chan, D. Y. C. & Thoroddsen, S. T. Stabilization of Leidenfrost vapour layer by textured superhydrophobic surfaces. *Nature* **489**, 274-277 (2012).

18 Jiang, M. *et al.* Inhibiting the Leidenfrost effect above 1,000 ° C for sustained thermal cooling. *Nature* **601**, 568-572 (2022).

19 Xu, M., Sun, G. & Kim, C.-J. Infinite lifetime of underwater superhydrophobic states. *Phys. Rev. Lett.* **113**, 136103 (2014).

20 Narhe, R. D. & Beysens, D. A. Nucleation and growth on a superhydrophobic grooved surface.

Phys. Rev. Lett. **93**, 076103 (2004).

21 Tian, X., Verho, T. & Ras, R. H. A. Moving superhydrophobic surfaces toward real-world applications. *Science* **352**, 142-143 (2016).

22 Wang, D. *et al.* Design of robust superhydrophobic surfaces. *Nature* **582**, 55-59 (2020).

23 Nosonovsky, M. Slippery when wetted. *Nature* **477**, 412-413 (2011).

24 Chen, X., Wen, G. & Guo, Z. What are the design principles, from the choice of lubricants and structures to the preparation method, for a stable slippery lubricant-infused porous surface? *Mater. Horiz.* **7**, 1697-1726 (2020).

25 Peppou-Chapman, S., Hong, J. K., Waterhouse, A. & Neto, C. Life and death of liquid-infused surfaces: a review on the choice, analysis and fate of the infused liquid layer. *Chem. Soc. Rev.* **49**, 3688-3715 (2020).

26 Buddingh, J. V., Hozumi, A. & Liu, G. Liquid and liquid-like surfaces/coatings that readily slide fluids. *Prog. Polym. Sci.* **123**, 101468 (2021).

27 Krumpfer, J. W. & McCarthy, T. J. Contact angle hysteresis: a different view and a trivial recipe for low hysteresis hydrophobic surfaces. *Faraday Discuss.* **146**, 103-111 (2010).

28 Wooh, S. & Vollmer, D. Silicone brushes: omniphobic surfaces with low sliding angles. *Angew. Chem. Int. Ed.* **55**, 6822-6824 (2016).

29 Gao, L. & McCarthy, T. J. Contact angle hysteresis explained. *Langmuir* **22**, 6234-6237 (2006).

30 Chen, W. *et al.* Ultrahydrophobic and ultralyophobic surfaces: some comments and examples. *Langmuir* **15**, 3395-3399 (1999).

31 Daniel, D. *et al.* Origins of extreme liquid repellency on structured, flat, and lubricated hydrophobic surfaces. *Phys. Rev. Lett.* **120**, 244503 (2018).

32 Armstrong, S., McHale, G., Ledesma-Aguilar, R. & Wells, G. G. Pinning-free evaporation of sessile droplets of water from solid surfaces. *Langmuir* **35**, 2989-2996 (2019).

33 Barrio-Zhang, H. *et al.* Contact-angle hysteresis and contact-line friction on slippery liquid-like surfaces. *Langmuir* **36**, 15094-15101 (2020).

34 Fang, L. *et al.* High‐resolution patterned functionalization of slippery “liquid‐like” brush surfaces via microdroplet‐confined growth of multifunctional polydopamine arrays. *Adv. Funct. Mater.* **31**, 2100447 (2021).

35 Fan, Y. *et al.* Reducing the contact time of impacting water drops on superhydrophobic surfaces by liquid-like coatings. *Chem. Eng. J.* **448**, 137638 (2022).

36 Young, T. III. An essay on the cohesion of fluids. *Philos. Trans. R. Soc. London*, 65-87 (1805).

37 Huhtamäki, T., Tian, X., Korhonen, J. T. & Ras, R. H. A. Surface-wetting characterization using contact-angle measurements. *Nat. Protoc.* **13**, 1521-1538 (2018).

38 Marmur, A. Solid-surface characterization by wetting. *Annu. Rev. Mater. Res.* **39**, 473-489 (2009).

39 Law, K.-Y. Contact angle hysteresis on smooth/flat and rough surfaces. Interpretation, mechanism, and origin. *Acc. Mater. Res.* **3**, 1-7 (2021).

40 Perrin, H., Lhermerout, R., Davitt, K., Rolley, E. & Andreotti, B. Defects at the nanoscale impact contact line motion at all scales. *Phys. Rev. Lett.* **116**, 184502 (2016).

41 Giacomello, A., Schimmele, L. & Dietrich, S. Wetting hysteresis induced by nanodefects. *PNAS* **113**, E262-E271 (2016).

42 McHale, G., Gao, N., Wells, G. G., Barrio-Zhang, H. & Ledesma-Aguilar, R. Friction

coefficients for droplets on solids: the liquid‑solid Amontons' laws. *Langmuir* **38**, 4425-4433 (2022).

43 Gao, N. *et al.* How drops start sliding over solid surfaces. *Nat. Phys.* **14**, 191-196 (2018).

44 Snoeijer, J. H. & Andreotti, B. Moving contact lines: scales, regimes, and dynamical transitions. *Annu. Rev. Fluid Mech.* **45**, 269-292 (2013).

45 Ritsema van Eck, G. C., Chiappisi, L. & de Beer, S. Fundamentals and applications of polymer brushes in air. *ACS Appl. Polym. Mater.* **4**, 3062-3087 (2022).

46 Ulman, A. Formation and structure of self-assembled monolayers. *Chem. Rev.* **96**, 1533-1554 (1996).

47 Jones, R. A. L. Glasses with liquid-like surfaces. *Nat. Mater.* **2**, 645-646 (2003).

48 Fakhraai, Z. & Forrest, J. A. Measuring the surface dynamics of glassy polymers. *Science* **319**, 600-604 (2008).

49 Hao, Z. *et al.* Mobility gradients yield rubbery surfaces on top of polymer glasses. *Nature* **596**, 372-376 (2021).

50 Sperling, L. H. *Introduction to physical polymer science (4th ed.)*. pp 349-426 (John Wiley & Sons, 2006).

51 Cheng, D. F., Urata, C., Yagihashi, M. & Hozumi, A. A statically oleophilic but dynamically oleophobic smooth nonperfluorinated surface. *Angew. Chem.* **124**, 3010-3013 (2012).

52 Cheng, D. F., Masheder, B., Urata, C. & Hozumi, A. Smooth perfluorinated surfaces with different chemical and physical natures: their unusual dynamic dewetting behavior toward polar and nonpolar liquids. *Langmuir* **29**, 11322-11329 (2013).

53 Yarbrough, J. C. *et al.* Contact angle analysis, surface dynamics, and biofouling characteristics of cross-linkable, random perfluoropolyether-based graft terpolymers. *Macromolecules* **39**, 2521-2528 (2006).

54 Hozumi, A. & McCarthy, T. Ultralyophobic oxidized aluminum surfaces exhibiting negligible contact angle hysteresis. *Langmuir* **26**, 2567-2573 (2010).

55 Lhermerout, R., Perrin, H., Rolley, E., Andreotti, B. & Davitt, K. A moving contact line as a rheometer for nanometric interfacial layers. *Nat. Commun.* **7**, 1-6 (2016).

56 Rubinstein, M. & Colby, R. H. *Polymer physics*. Vol. 23, 49-96 (New York: Oxford university press 2003).

57 Longenberger, T. B., Ryan, K. M., Bender, W. Y., Krumpfer, A.-K. & Krumpfer, J. W. The art of silicones: bringing siloxane chemistry to the undergraduate curriculum. *J. Chem. Educ.* **94**, 1682-1690 (2017).

58 Zheng, P. & McCarthy, T. J. Rediscovering silicones: molecularly smooth, low surface energy, unfilled, UV/vis-transparent, extremely cross-linked, thermally stable, hard, elastic PDMS. *Langmuir* **26**, 18585-18590 (2010).

59 Krumpfer, J. W. & McCarthy, T. J. Rediscovering silicones: "unreactive" silicones react with inorganic surfaces. *Langmuir* **27**, 11514-11519 (2011).

60 Hamada, T. Rotational isomeric state study of molecular dimensions and elasticity of perfluoropolyethers: differences between Demnum-, Fomblin-, and Krytox-type main chains. *Phys. Chem. Chem. Phys.* **2**, 115-122 (2000).

61 Pauling, L. The nature of silicon‑oxygen bonds. *Am. Mineral.* **65**, 321-323 (1980).

62 Agapov, A. & Sokolov, A. P. Size of the dynamic bead in polymers. *Macromolecules* **43**, 9126-9130 (2010).

63 Singh, N. *et al.* Omniphobic metal surfaces with low contact angle hysteresis and tilt angles. *Langmuir* **34**, 11405-11413 (2018).

64 Cheng, D. F., Urata, C., Masheder, B. & Hozumi, A. A physical approach to specifically improve the mobility of alkane liquid drops. *J. Am. Chem. Soc.* **134**, 10191-10199 (2012).

65 Huang, Y. *et al.* A facile approach to fabricate dynamically omniphobic coating on diverse substrates for self-cleaning. *Prog. Org. Coat.* **132**, 475-480 (2019).

66 Gao, P. *et al.* Liquid-like transparent and flexible coatings for anti-graffiti applications. *Prog. Org. Coat.* **161**, 106476 (2021).

67 Zhang, G., Liang, B., Zhong, Z., Huang, Y. & Su, Z. One‐step solvent‐free strategy for covalently attached, substrate‐independent transparent slippery coating. *Adv. Mater. Interfaces* **5**, 1800646 (2018).

68 Brittain, W. J. & Minko, S. A structural definition of polymer brushes. *J. Polym. Sci. Part A: Polym. Chem.* **45**, 3505-3512 (2007).

69 Fadeev, A. Y. & McCarthy, T. J. Trialkylsilane monolayers covalently attached to silicon surfaces: wettability studies indicating that molecular topography contributes to contact angle hysteresis. *Langmuir* **15**, 3759-3766 (1999).

70 Scott, M. C., Stevens, D. R., Bochinski, J. R. & Clarke, L. I. Dynamics within alkylsiloxane self-assembled monolayers studied by sensitive dielectric spectroscopy. *ACS Nano* **2**, 2392-2400 (2008).

71 Urata, C., Cheng, D. F., Masheder, B. & Hozumi, A. Smooth, transparent and nonperfluorinated surfaces exhibiting unusual contact angle behavior toward organic liquids. *RSC Adv.* **2**, 9805-9808 (2012).

72 Urata, C., Masheder, B., Cheng, D. F. & Hozumi, A. How to reduce resistance to movement of alkane liquid drops across tilted surfaces without relying on surface roughening and perfluorination. *Langmuir* **28**, 17681-17689 (2012).

73 Urata, C., Masheder, B., Cheng, D. F. & Hozumi, A. Unusual dynamic dewetting behavior of smooth perfluorinated hybrid films: potential advantages over conventional textured and liquid-infused perfluorinated surfaces. *Langmuir* **29**, 12472-12482 (2013).

74 Lhermerout, R. & Davitt, K. Contact angle dynamics on pseudo-brushes: effects of polymer chain length and wetting liquid. *Colloids Surf. A* **566**, 148-155 (2019).

75 Flagg, D. H. & McCarthy, T. J. Rapid and clean covalent attachment of methylsiloxane polymers and oligomers to silica using $B(C_6F_5)_3$ catalysis. *Langmuir* **33**, 8129-8139 (2017).

76 Luap, C. & Goedel, W. A. Linear viscoelastic behavior of end-tethered polymer monolayers at the air/water interface. *Macromolecules* **34**, 1343-1351 (2001).

77 Wang, L. & McCarthy, T. J. Covalently attached liquids: instant omniphobic surfaces with unprecedented repellency. *Angew. Chem. Int. Ed.* **55**, 244-248 (2016).

78 Wooh, S. & Butt, H. J. A photocatalytically active lubricant‐impregnated surface. *Angew. Chem. Int. Ed.* **129**, 5047-5051 (2017).

79 Wooh, S., Encinas, N., Vollmer, D. & Butt, H. J. Stable hydrophobic metal‐oxide photocatalysts via grafting polydimethylsiloxane brush. *Adv. Mater.* **29**, 1604637 (2017).

80 Teisala, H., Baumli, P., Weber, S. A. L., Vollmer, D. & Butt, H.-J. Grafting silicone at room temperature—a transparent, scratch-resistant nonstick molecular coating. *Langmuir* **36**, 4416-4431 (2020).

81 Liu, P. *et al.* Development of “liquid-like” copolymer nanocoatings for reactive oil-

repellent surface. *ACS Nano* 11, 2248-2256 (2017).

82 Yu, M. *et al.* Covalently grafted liquids for transparent and omniphobic surfaces via thiol-ene click chemistry. *J. Mater. Sci.* 55, 12811-12825 (2020).

83 Liu, J. *et al.* One‐step synthesis of a durable and liquid‐repellent poly(dimethylsiloxane) coating. *Adv. Mater.* 33, 2100237 (2021).

84 Zhang, L., Guo, Z., Sarma, J. & Dai, X. Passive removal of highly wetting liquids and ice on quasi-liquid surfaces. *ACS Appl. Mater. Interfaces* 12, 20084-20095 (2020).

85 Zhao, X., Khandoker, M. A. R. & Golovin, K. Non-fluorinated omniphobic paper with ultralow contact angle hysteresis. *ACS Appl. Mater. Interfaces* 12, 15748-15756 (2020).

86 Khatir, B., Shabanian, S. & Golovin, K. Design and high-resolution characterization of silicon wafer-like omniphobic liquid layers applicable to any substrate. *ACS Appl. Mater. Interfaces* 12, 31933-31939 (2020).

87 Huang, S., Li, J., Liu, L., Zhou, L. & Tian, X. Lossless fast drop self‐transport on anisotropic omniphobic surfaces: origin and elimination of microscopic liquid residue. *Adv. Mater.* 31, 1901417 (2019).

88 Soltani, M. & Golovin, K. Lossless, passive transportation of low surface tension liquids induced by patterned omniphobic liquidlike polymer brushes. *Adv. Funct. Mater.* 32, 2107465 (2022).

89 Kaneko, S., Urata, C., Sato, T., Hönes, R. & Hozumi, A. Smooth and transparent films showing paradoxical surface properties: the lower the static contact angle, the better the water sliding performance. *Langmuir* 35, 6822-6829 (2019).

90 Cha, H. *et al.* Dropwise condensation on solid hydrophilic surfaces. *Sci. Adv.* 6, eaax0746 (2020).

91 Papra, A., Gadegaard, N. & Larsen, N. B. Characterization of ultrathin poly(ethylene glycol) monolayers on silicon substrates. *Langmuir* 17, 1457-1460 (2001).

92 Zhong, X., Hu, H., Yang, L., Sheng, J. & Fu, H. Robust hyperbranched polyester-based anti-smudge coatings for self-cleaning, anti-graffiti, and chemical shielding. *ACS Appl. Mater. Interfaces* 11, 14305-14312 (2019).

93 Yang, J., Li, J., Jia, X., Li, Y. & Song, H. Fabrication of robust and transparent slippery coating with hot water repellency, antifouling property, and corrosion resistance. *ACS Appl. Mater. Interfaces* 12, 28645-28654 (2020).

94 Wei, D., Zeng, J. & Yong, Q. High-performance bio-based polyurethane antismudge coatings using castor oil-based hyperbranched polyol as superior cross-linkers. *ACS Appl. Polym. Mater.* 3, 3612-3622 (2021).

95 Zhong, X., Lv, L., Hu, H., Jiang, X. & Fu, H. Bio-based coatings with liquid repellency for various applications. *Chem. Eng. J.* 382, 123042 (2020).

96 Yu, L., Chen, G. Y., Xu, H. & Liu, X. Substrate-independent, transparent oil-repellent coatings with self-healing and persistent easy-sliding oil repellency. *ACS Nano* 10, 1076-1085 (2016).

97 Huang, S. *et al.* Water-based anti-smudge NP-GLIDE polyurethane coatings. *Chem. Eng. J.* 351, 210-220 (2018).

98 Hu, H., Liu, G. & Wang, J. Clear and durable epoxy coatings that exhibit dynamic omniphobicity. *Adv. Mater. Interfaces* 3, 1600001 (2016).

99 Lei, L., Buddingh, J., Wang, J. & Liu, G. Transparent omniphobic polyurethane coatings

containing partially acetylated β‑cyclodextrin as the polyol. *Chem. Eng. J.* **380**, 122554 (2020).

100 Rabnawaz, M., Liu, G. & Hu, H. Fluorine‑free anti‑smudge polyurethane coatings. *Angew. Chem. Int. Ed.* **127**, 12913-12918 (2015).

101 Rabnawaz, M. & Liu, G. Graft‑copolymer‑based approach to clear, durable, and anti-smudge polyurethane coatings. *Angew. Chem. Int. Ed.* **54**, 6516-6520 (2015).

102 Xu, F., Li, X., Weng, D., Li, Y. & Sun, J. Transparent antismudge coatings with thermally assisted healing ability. *J. Mater. Chem. A* **7**, 2812-2820 (2019).

103 Ma, J. *et al.* Ultra-thin self-healing vitrimer coatings for durable hydrophobicity. *Nat. Commun.* **12**, 1-10 (2021).

104 Musil, J. Flexible hard nanocomposite coatings. *RSC Adv.* **5**, 60482-60495 (2015).

105 Sanchez, C., Arribart, H. & Giraud Guille, M. M. Biomimetism and bioinspiration as tools for the design of innovative materials and systems. *Nat. Mater.* **4**, 277-288 (2005).

106 Boban, M. *et al.* Smooth, all-solid, low-hysteresis, omniphobic surfaces with enhanced mechanical durability. *ACS Appl. Mater. Interfaces* **10**, 11406-11413 (2018).

107 Bender, D. N., Zhang, K., Wang, J. & Liu, G. Hard yet flexible transparent omniphobic GPOSS coatings modified with perfluorinated agents. *ACS Appl. Mater. Interfaces* **13**, 10467-10479 (2021).

108 Zhang, K., Huang, S., Wang, J. & Liu, G. Transparent organic/silica nanocomposite coating that is flexible, omniphobic, and harder than a 9H pencil. *Chem. Eng. J.* **396**, 125211 (2020).

109 Choi, G. M. *et al.* Flexible hard coating: glass‑like wear resistant, yet plastic‑like compliant, transparent protective coating for foldable displays. *Adv. Mater.* **29**, 1700205 (2017).

110 Zhang, K., Huang, S., Wang, J. & Liu, G. Transparent omniphobic coating with glass‑like wear resistance and polymer‑like bendability. *Angew. Chem. Int. Ed.* **58**, 12004-12009 (2019).

111 Zheng, W. *et al.* Judicious design and rapid manufacturing of flexible, mechanically resistant liquid-like coating with strong bonding and antifouling abilities. *Adv. Mater.*, doi:10.1002/adma.202204581 (2022).

112 Lai, Z. & Liu, G. Facile preparation of a transparent and rollable omniphobic coating with exceptional hardness and wear resistance. *ACS Appl. Mater. Interfaces* **14**, 35138-35147 (2022).

113 Urata, C., Masheder, B., Cheng, D. F. & Hozumi, A. A thermally stable, durable and temperature-dependent oleophobic surface of a polymethylsilsesquioxane film. *Chem. Commun.* **49**, 3318-3320 (2013).

114 Gao, P. *et al.* Rational design of durable anti-fouling coatings with high transparency, hardness, and flexibility. *ACS Appl. Mater. Interfaces* **14**, 29156-29166 (2022).

115 Wang, Y. *et al.* Liquid‑like SiO_2‑*g*‑PDMS coatings on wood surfaces with underwater durability, antifouling, antismudge, and self‑healing properties. *Adv. Sustainable Syst.* **3**, 1800070 (2019).

116 Wang, Y. & He, J. Fabrication of ultra-smooth hybrid thin coatings towards robust, highly transparent, liquid-repellent and antismudge coatings. *J. Colloid Interface Sci.* **594**, 781-790 (2021).

117 Zhang, L., Guo, Z., Sarma, J., Zhao, W. & Dai, X. Gradient quasi‑liquid surface enabled self‑propulsion of highly wetting liquids. *Adv. Funct. Mater.* **31**, 2008614 (2021).

118 Yang, C. *et al.* Liquid-like polymer-based self-cleaning coating for effective prevention of

liquid foods contaminations. *J. Colloid Interface Sci.* **589**, 327-335 (2021).

119 Zheng, C., Liu, G. & Hu, H. UV-curable antismudge coatings. *ACS Appl. Mater. Interfaces* **9**, 25623-25630 (2017).

120 Zhong, X., Sheng, J. & Fu, H. A novel UV/sunlight-curable anti-smudge coating system for various substrates. *Chem. Eng. J.* **345**, 659-668 (2018).

121 Gee, E., Liu, G., Hu, H. & Wang, J. Effect of varying chain length and content of poly(dimethylsiloxane) on dynamic dewetting performance of NP-GLIDE polyurethane coatings. *Langmuir* **34**, 10102-10113 (2018).

122 Masheder, B., Urata, C. & Hozumi, A. Transparent and hard zirconia-based hybrid coatings with excellent dynamic/thermoresponsive oleophobicity, thermal durability, and hydrolytic stability. *ACS Appl. Mater. Interfaces* **5**, 7899-7905 (2013).

123 Wu, C. *et al.* Whether and when superhydrophobic/superoleophobic surfaces are fingerprint repellent. *Research* **2022**, 9850316 (2022).

124 Wu, Q. *et al.* Slippery liquid-attached surface for robust biofouling resistance. *ACS Biomater. Sci. Eng.* **6**, 358-366 (2019).

125 Zhu, Y. *et al.* Slippery liquid-like solid surfaces with promising antibiofilm performance under both static and flow conditions. *ACS Appl. Mater. Interfaces* **14**, 6307-6319 (2022).

126 Yang, C. *et al.* Liquid-like polymer coating as a promising candidate for reducing electrode contamination and noise in complex biofluids. *ACS Appl. Mater. Interfaces* **13**, 4450-4462 (2021).

127 Wu, Q. *et al.* Liquid-like layer coated intraocular lens for posterior capsular opacification prevention. *Appl. Mater. Today* **23**, 100981 (2021).

128 Hao, X. *et al.* Self-lubricative organic–inorganic hybrid coating with anti-icing and anti-waxing performances by grafting liquid-like polydimethylsiloxane. *Adv. Mater. Interfaces* **9** (2022).

129 Ouyang, M. *et al.* Ultralow-adhesion icephobic surfaces: combining superhydrophobic and liquid-like properties in the same surface. *Nano Res.*, doi:10.1007/s12274-022-4746-z (2022).

130 Zheng, H., Liu, G., Nienhaus, B. B. & Buddingh, J. V. Ice-shedding polymer coatings with high hardness but low ice adhesion. *ACS Appl. Mater. Interfaces* **14**, 6071-6082 (2022).

131 Zhao, X. *et al.* Macroscopic evidence of the liquidlike nature of nanoscale polydimethylsiloxane brushes. *ACS Nano* **15**, 13559-13567 (2021).

132 Sarma, J., Zhang, L., Guo, Z. & Dai, X. Sustainable icephobicity on durable quasi-liquid surface. *Chem. Eng. J.* **431** (2022).

133 Halvey, A. K. *et al.* Rapid and robust surface treatment for simultaneous solid and liquid repellency. *ACS Appl. Mater. Interfaces* **13**, 53171-53180 (2021).

134 Newby, B.-m. Z., Chaudhury, M. K. & Brown, H. R. Macroscopic evidence of the effect of interfacial slippage on adhesion. *Science* **269**, 1407-1409 (1995).

135 Meng, J. & Wang, S. Advanced antiscaling interfacial materials toward highly efficient heat energy transfer. *Adv. Funct. Mater.* **30**, 1904796 (2020).

136 Chen, Y. *et al.* Dynamic poly(dimethylsiloxane) brush coating shows even better antiscaling capability than the low-surface-energy fluorocarbon counterpart. *Environ. Sci. Technol.* **55**, 8839-8847 (2021).

137 Zhao, H. *et al.* Extreme antiscaling performance of slippery omniphobic covalently attached liquids. *ACS Appl. Mater. Interfaces* **12**, 12054-12067 (2020).

138 Zhao, H. *et al.* Scalable slippery omniphobic covalently attached liquid coatings for flow fouling reduction. *ACS Appl. Mater. Interfaces* **13**, 38666-38679 (2021).

139 Lin, S., Li, B., Xu, Y., Mehrizi, A. A. & Chen, L. Effective strategies for droplet transport on solid surfaces. *Adv. Mater. Interfaces* **8**, 2001441 (2021).

140 Monga, D. *et al.* Quasi-liquid surfaces for sustainable high-performance steam condensation. *ACS Appl. Mater. Interfaces* **14**, 13932-13941 (2022).

141 Baidya, A., Das, S. K. & Pradeep, T. An aqueous composition for lubricant-free, robust, slippery, transparent coatings on diverse substrates. *Global Challenges* **2**, 1700097 (2018).

142 Li, J. *et al.* Oil droplet self-transportation on oleophobic surfaces. *Sci. Adv.* **2**, e1600148 (2016).

143 Wang, X., Wang, Z., Heng, L. & Jiang, L. Stable omniphobic anisotropic covalently grafted slippery surfaces for directional transportation of drops and bubbles. *Adv. Funct. Mater.* **30**, 1902686 (2020).

144 Huang, S., Li, J., Chen, L. & Tian, X. Suppressing the universal occurrence of microscopic liquid residues on super-liquid-repellent surfaces. *J. Phys. Chem. Lett.* **12**, 3577-3585 (2021).

145 Wang, Z., Wang, Y. & Liu, G. Rapid and efficient separation of oil from oil-in-water emulsions using a Janus cotton fabric. *Angew. Chem. Int. Ed.* **55**, 1291-1294 (2016).

146 Liu, Y., Wang, X. & Feng, S. Nonflammable and magnetic sponge decorated with polydimethylsiloxane brush for multitasking and highly efficient oil-water separation. *Adv. Funct. Mater.* **29** (2019).

147 Chen, L. *et al.* A grafted-liquid lubrication strategy to enhance membrane permeability in viscous liquid separation. *J. Membr. Sci.* **610**, 118240 (2020).

148 Liu, S. *et al.* A strategy of liquid-grafted slippery sponges with simultaneously enhanced absorption and desorption performances for crude oil spill remediation. *Macromol. Mater. Eng.* **306**, 2100242 (2021).

149 Huang, Y.-X., Liang, D.-Q., Luo, C.-H., Zhang, Y. & Meng, F. Liquid-like surface modification for effective anti-scaling membrane distillation with uncompromised flux. *J. Membr. Sci.* **637**, 119673 (2021).

150 Liu, D., Cao, J., Qiu, M., Zhang, G. & Hong, Y. Enhanced properties of PVDF nanofibrous membrane with liquid-like coating for membrane distillation. *Sep. Purif. Technol.* **295**, 121282 (2022).

151 Bourlinos, A. B. *et al.* Silicone-functionalized carbon nanotubes for the production of new carbon-based fluids. *Carbon* **45**, 1583-1585 (2007).

Highlighted references

26 Buddingh, J. V., Hozumi, A. & Liu, G. Liquid and liquid-like surfaces/coatings that readily slide fluids. *Prog. Polym. Sci.* **123**, 101468 (2021).

An introductory overview on slippery liquid-infused surfaces and liquid-like surfaces.

27 Krumpfer, J. W. & McCarthy, T. J. Contact angle hysteresis: a different view and a trivial recipe for low hysteresis hydrophobic surfaces. *Faraday Discuss.* **146**, 103-111 (2010).

A pioneering example of PDMS-grafted surfaces featuring liquid-like nature and low hysteresis.

30 Chen, W. *et al.* Ultrahydrophobic and ultralyophobic surfaces: some comments and examples. *Langmuir* **15**, 3395-3399 (1999).

A pioneering example of smooth alkylsilane monolayer featuring liquid-like nature and low

hysteresis.

51 Cheng, D. F., Urata, C., Yagihashi, M. & Hozumi, A. A statically oleophilic but dynamically oleophobic smooth nonperfluorinated surface. *Angew. Chem.* **124**, 3010-3013 (2012).

Study demonstrating the dynamic omniphobic mechanism of liquid-like surfaces.

52 Cheng, D. F., Masheder, B., Urata, C. & Hozumi, A. Smooth perfluorinated surfaces with different chemical and physical natures: their unusual dynamic dewetting behavior toward polar and nonpolar liquids. *Langmuir* **29**, 11322-11329 (2013).

A pioneering example of PFPE-grafted surface featuring liquid-like nature and low hysteresis.

64 Cheng, D. F., Urata, C., Masheder, B. & Hozumi, A. A physical approach to specifically improve the mobility of alkane liquid drops. *J. Am. Chem. Soc.* **134**, 10191-10199 (2012).

Study demonstrating the effect of chain length on liquid-like nature.

77 Wang, L. & McCarthy, T. J. Covalently attached liquids: instant omniphobic surfaces with unprecedented repellency. *Angew. Chem. Int. Ed.* **55**, 244-248 (2016).

Report of a simple, rapid graft-from approach to prepare liquid-like PDMS brushes.

87 Huang, S., Li, J., Liu, L., Zhou, L. & Tian, X. Lossless fast drop self‐transport on anisotropic omniphobic surfaces: origin and elimination of microscopic liquid residue. *Adv. Mater.* **31**, 1901417 (2019).

Report of a truly lossless fast droplet self‐transport surface integrating anisotropic microstructure with liquid-like PFPE coating.

89 Kaneko, S., Urata, C., Sato, T., Hönes, R. & Hozumi, A. Smooth and transparent films showing paradoxical surface properties: the lower the static contact angle, the better the water sliding performance. *Langmuir* **35**, 6822-6829 (2019).

A pioneering example of PEG-grafted surface featuring statically hydrophilic but dynamically hydrophobic properties.

110 Zhang, K., Huang, S., Wang, J. & Liu, G. Transparent omniphobic coating with glass‐like wear resistance and polymer‐like bendability. *Angew. Chem. Int. Ed.* **58**, 12004-12009 (2019).

Report of a durable hard-yet-flexible liquid-like coating that could resist the wear of steel wool.

131 Zhao, X. *et al.* Macroscopic evidence of the liquidlike nature of nanoscale polydimethylsiloxane brushes. *ACS Nano* **15**, 13559-13567 (2021).

Study providing the macroscopic evidences of liquid-like nature of PDMS brushes.

Acknowledgements

L.C., S.H., and X.T. acknowledge the financial support from the National Natural Science Foundation of China (22072185, 21872176, and 12072381), the Guangdong Basic and Applied Basic Research Foundation (2021A1515110221), the Pearl River Talents Program (2017GC010671), and the Natural Science Foundation of Guangdong Province (2019A1515012030). R.H.A.R. acknowledges funding from the Academy of Finland Center of Excellence Program (2022-2029) in Life-Inspired Hybrid Materials (LIBER) (project number 346109) and Academy Project (project number 342169) and from the European Research Council for funding the Consolidator Grant SuperRepel (grant agreement no. 725513).

Author contributions

L.C. wrote and edited the article. S.H., X.T. and R.H.A.R. contributed to the discussion of content and edited the manuscript before submission.

Competing interests

The authors declare no competing interests.

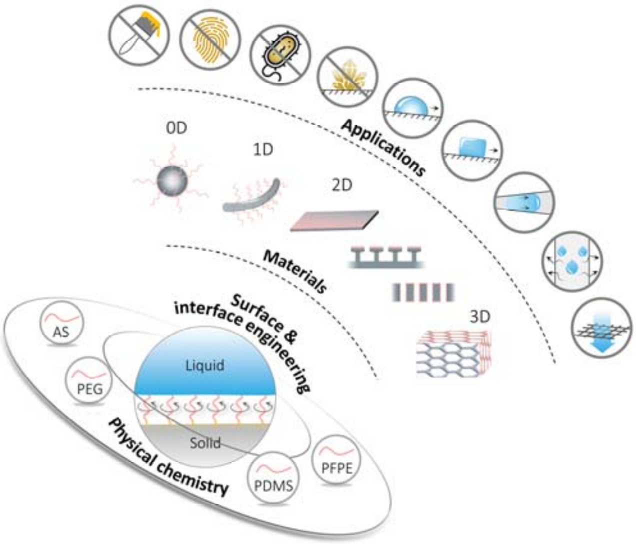

Graphical abstract

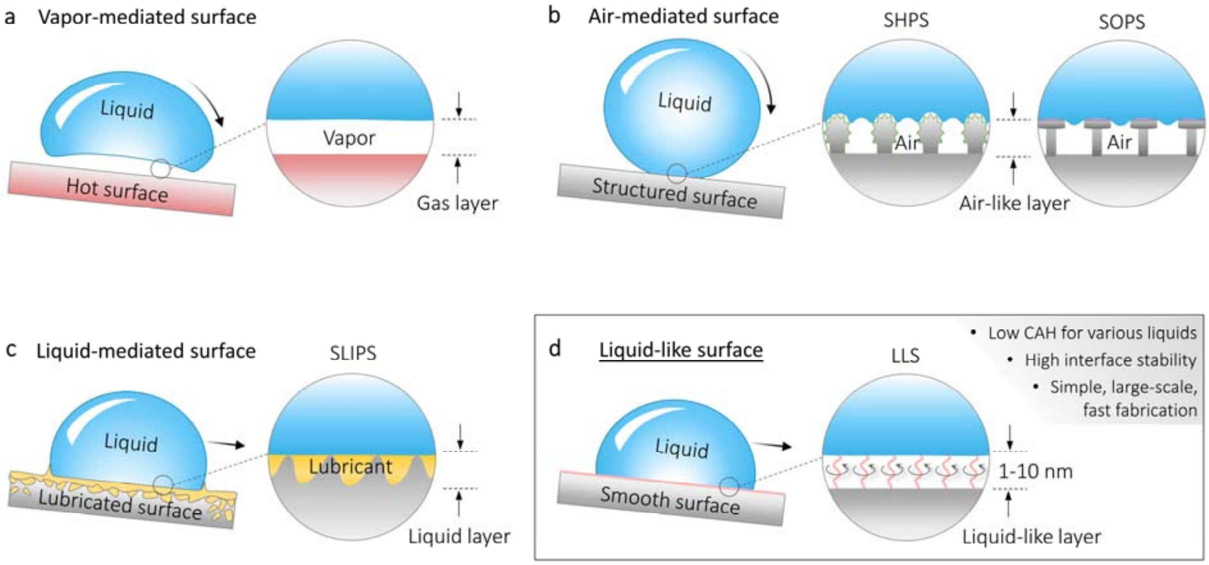

Fig. 1 Four types of liquid-repellent surfaces based on different design principles. (a) Vapor-mediated surface. When placing a droplet on a hot solid surface, a gas layer is generated by its vapor and the droplet can drift on the surface, known as the Leidenfrost phenomenon. (b) Air-mediated surface. Relying on specific surface structure and chemistry, droplets can sit atop surface microstructures, and an air-like layer is formed, for which the surfaces show high θ_0 and low θ_{roll} towards water or even oils. (c) Liquid-mediated surface. By infusing liquid lubricant into the porous surface, an extremely smooth and slippery liquid layer is formed on the surface, so that any immiscible liquids can readily slide off. (d) Liquid-like surface. By simple chemical grafting of highly mobile molecules onto the smooth solid surface, a liquid-like layer is formed and such surface exhibits ultralow CAH for various liquids.

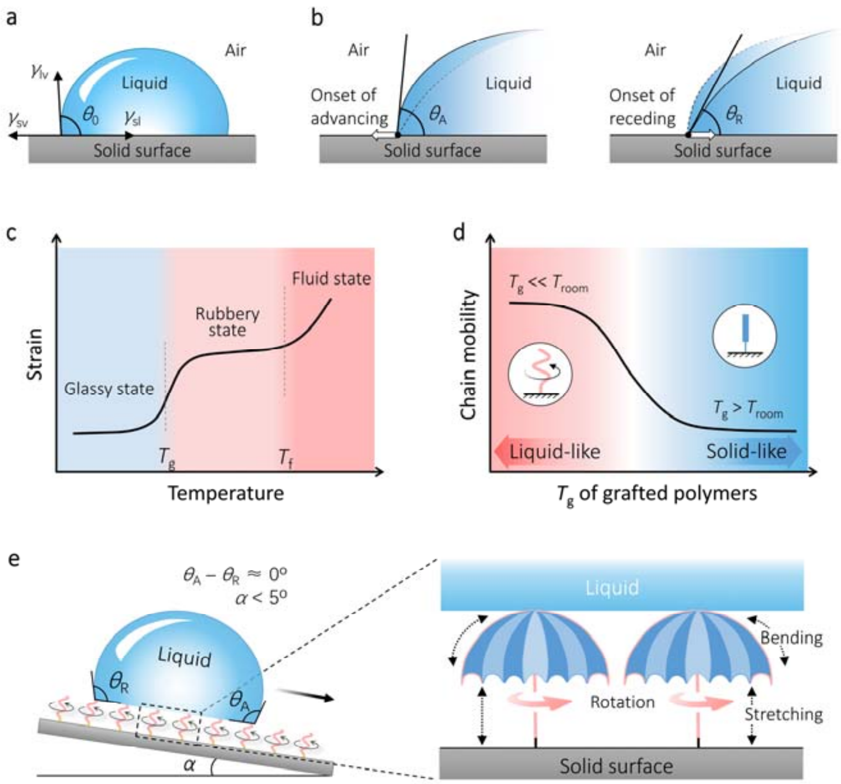

Fig. 2 Dynamics and thermodynamics of omniphobic LLSs. (a) Wetting model of a droplet settled on a smooth solid surface. (b) Hysteresis model indicating the onset of advancing and receding of three-phase contact line at θ_A and θ_R, respectively. (c) Classical thermo-mechanical curve of bulk amorphous polymers. (d) Chain mobility of polymers with different T_g when grafted on surfaces. (e) An "umbrella model" illustrating the high mobility of surface-grafted polymer chains. Panels (e) is adapted with permission from ref.[54], ACS.

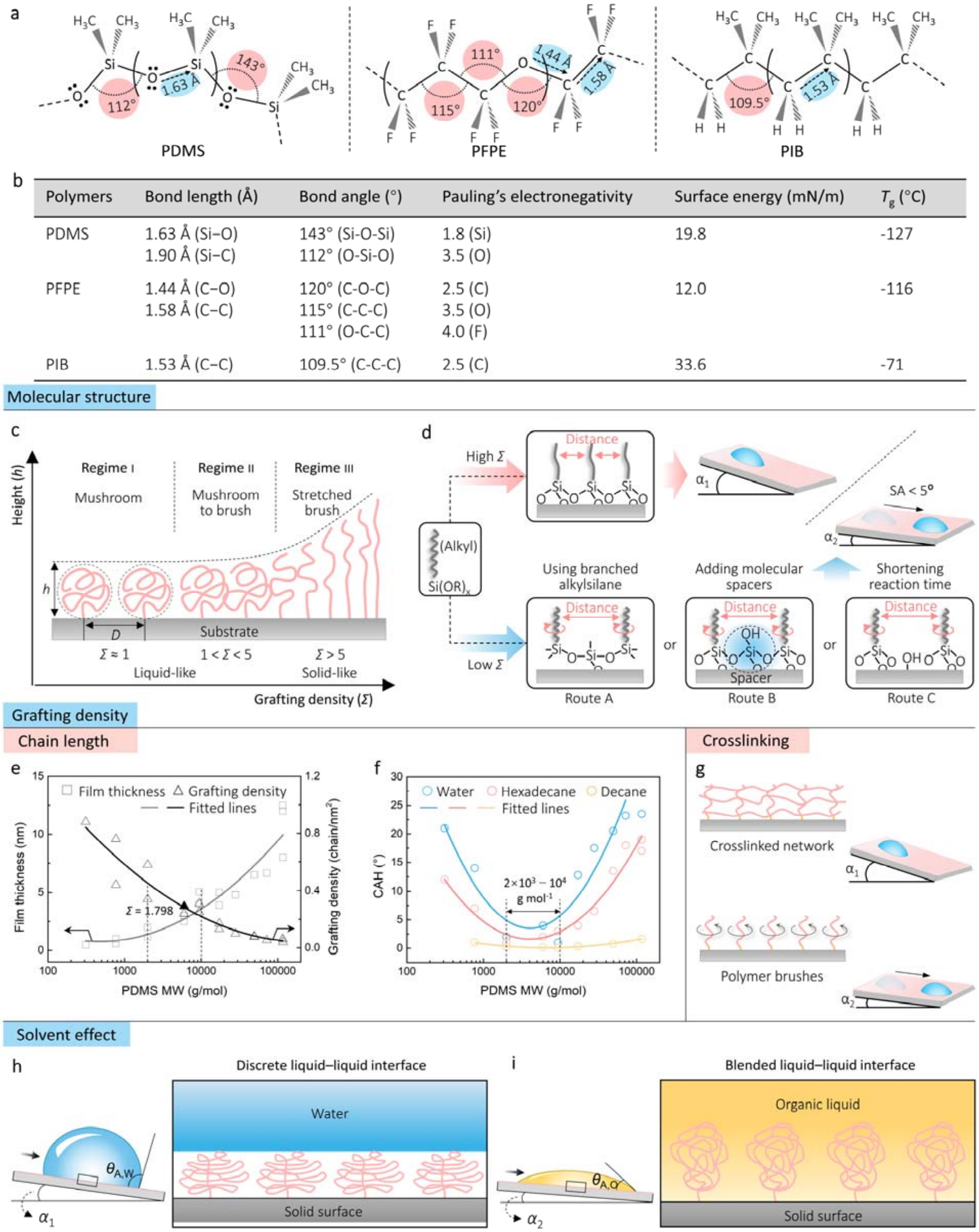

Polymers	Bond length (Å)	Bond angle (°)	Pauling's electronegativity	Surface energy (mN/m)	T_g (°C)
PDMS	1.63 Å (Si–O) 1.90 Å (Si–C)	143° (Si-O-Si) 112° (O-Si-O)	1.8 (Si) 3.5 (O)	19.8	-127
PFPE	1.44 Å (C–O) 1.58 Å (C–C)	120° (C-O-C) 115° (C-C-C) 111° (O-C-C)	2.5 (C) 3.5 (O) 4.0 (F)	12.0	-116
PIB	1.53 Å (C–C)	109.5° (C-C-C)	2.5 (C)	33.6	-71

Fig. 3 Influential factors on chain mobility. (a) Molecular structures of PDMS, PFPE, and PIB. (b) Comparison of bond length, bond angle, Pauling's electronegativity, surface energy and T_g of PDMS, PFPE, and PIB. (c) Regime transition diagram of surface-grafted polymer chains from "mushroom" regime ($\Sigma \approx 1$) to "mushroom-to-brush" ($1 < \Sigma < 5$) regime to "stretching brush" ($\Sigma > 5$) regime with an increasing grafting density gradient. (d)

Strategies to reduce the grafting density to improve the chain mobility of grafted alkyl groups. (e) Variation of the thickness and the grafting density of grafted PDMS brush layer with the MW of PDMS. (f) Change in CAH values for water, hexadecane, and decane on PDMS-grafted surfaces with increasing MW. (g) Effect of crosslinking on chain mobility. (h) Water and (i) organic liquid droplets resting on a PDMS-grafted LLS, corresponding to two different LLS-liquid interfaces. Panels (a) and (b) are adapted with permission from ref.[57], ACS. The data in graphs (e) and (f) are extracted from ref.[59,64,74]. Panels (h) and (i) are adapted with permission from ref.[28], Wiley.

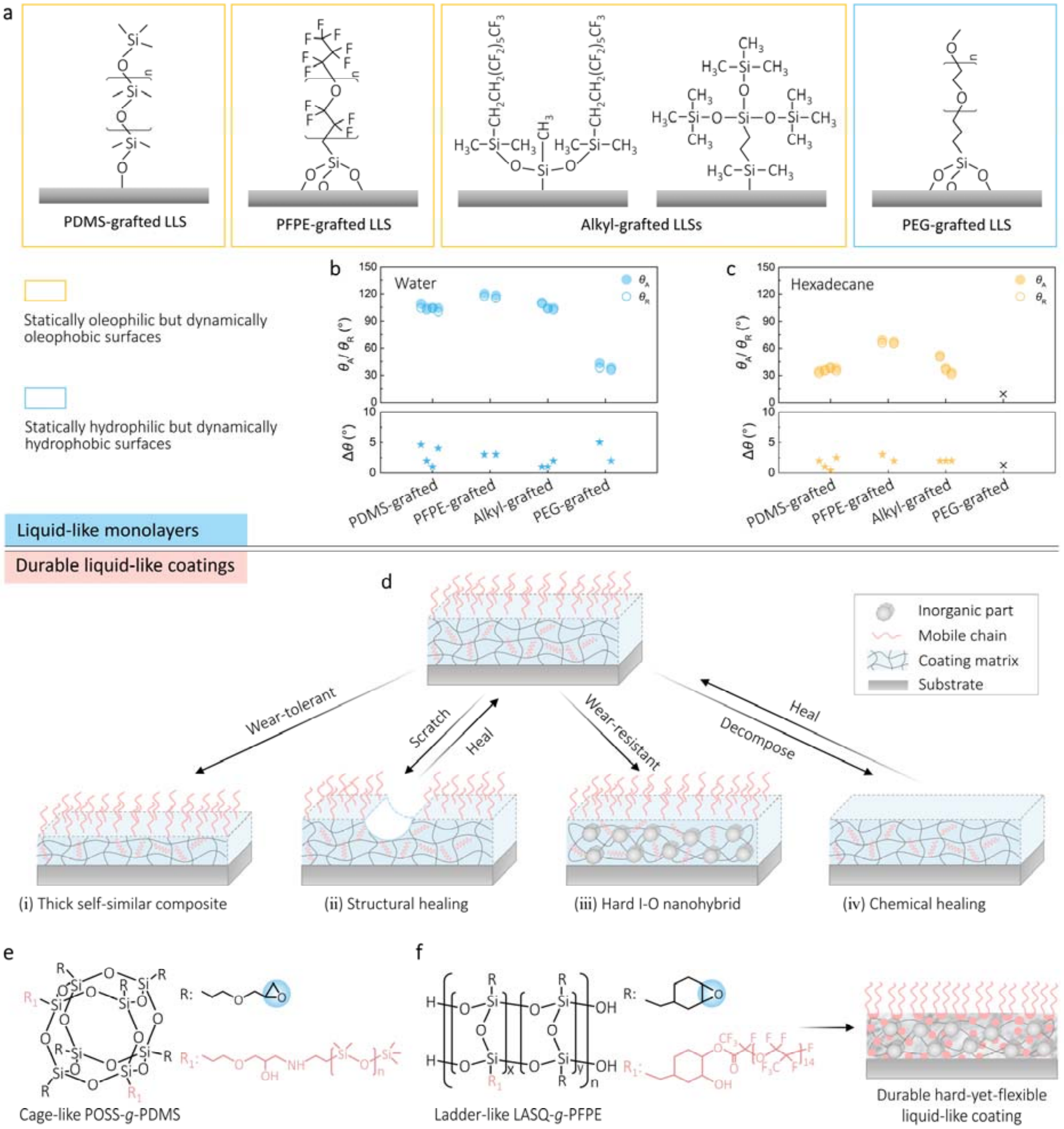

Fig. 4 Design of liquid-like monolayers and durable liquid-like coatings. (a) Four types of LLSs, including PDMS-grafted, PFPE-grafted, alkyl-grafted, and PEG-grafted LLSs. (b) Water and (c) hexadecane contact angles and CAH on four LLSs. The data in graphs (b) and (c) are extracted from ref.[30,51,54,59,77,87-90]. (d) Four strategies to design durable liquid-like coatings: (i) Thick self-similar composite for wear tolerance, (ii) Structural healing capacity, (iii) Hard I-O nanohybrid for wear resistance, and (iv) Chemical self-healing ability. (e) Copolymer of cage-like POSS bearing PDMS (POSS-*g*-PDMS) and (f) copolymer of ladder-like LASQ bearing PFPE (LASQ-*g*-PFPE) that are used to prepare durable hard-yet-flexible liquid-like coatings.

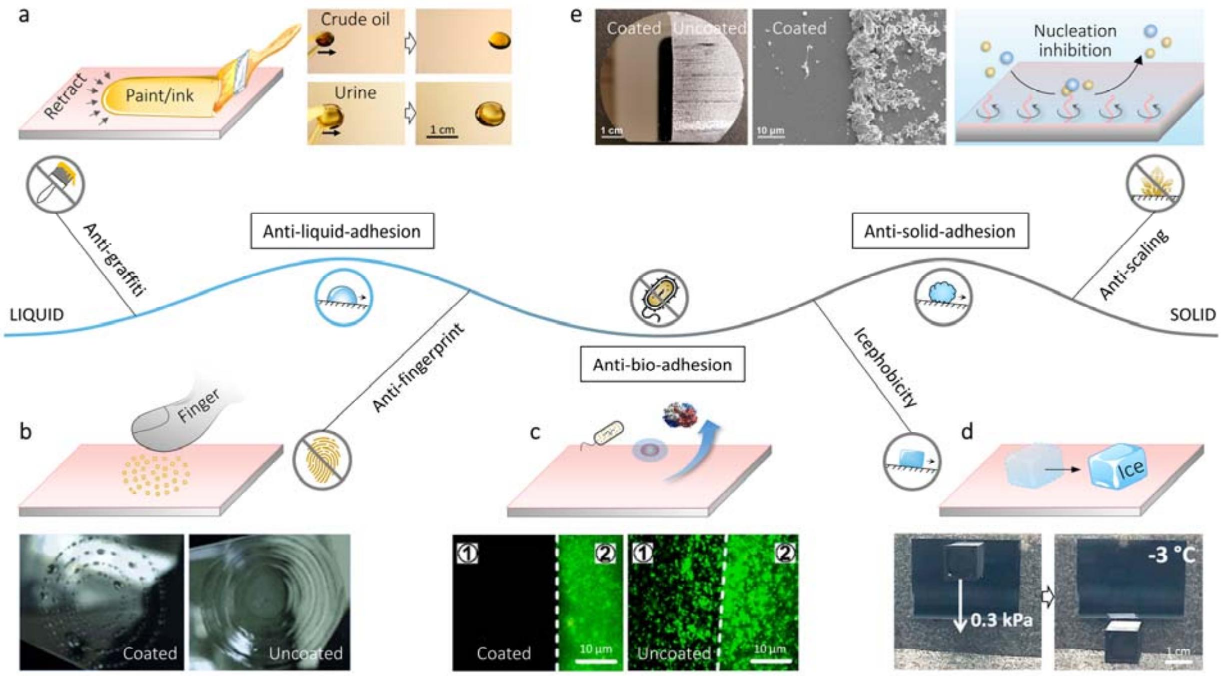

Fig. 5 Anti-liquid/bio/solid-adhesion applications of smooth LLSs. (a) Anti-graffiti ability against water- or oil-born ink, paint and marks. (b) Anti-fingerprint ability. (c) Anti-bioadhesion ability against bacteria, cells, and proteins. (d) Icephobicity for low ice adhesion strength. (e) Anti-scaling ability against the heterogeneous nucleation and growth of scale. The insets in panels (a)–(e) are separately adapted with permission from ref.[84], ACS; ref.[101], Wiley-VCH; ref.[124], ACS; ref.[131], ACS; ref.[137], ACS.

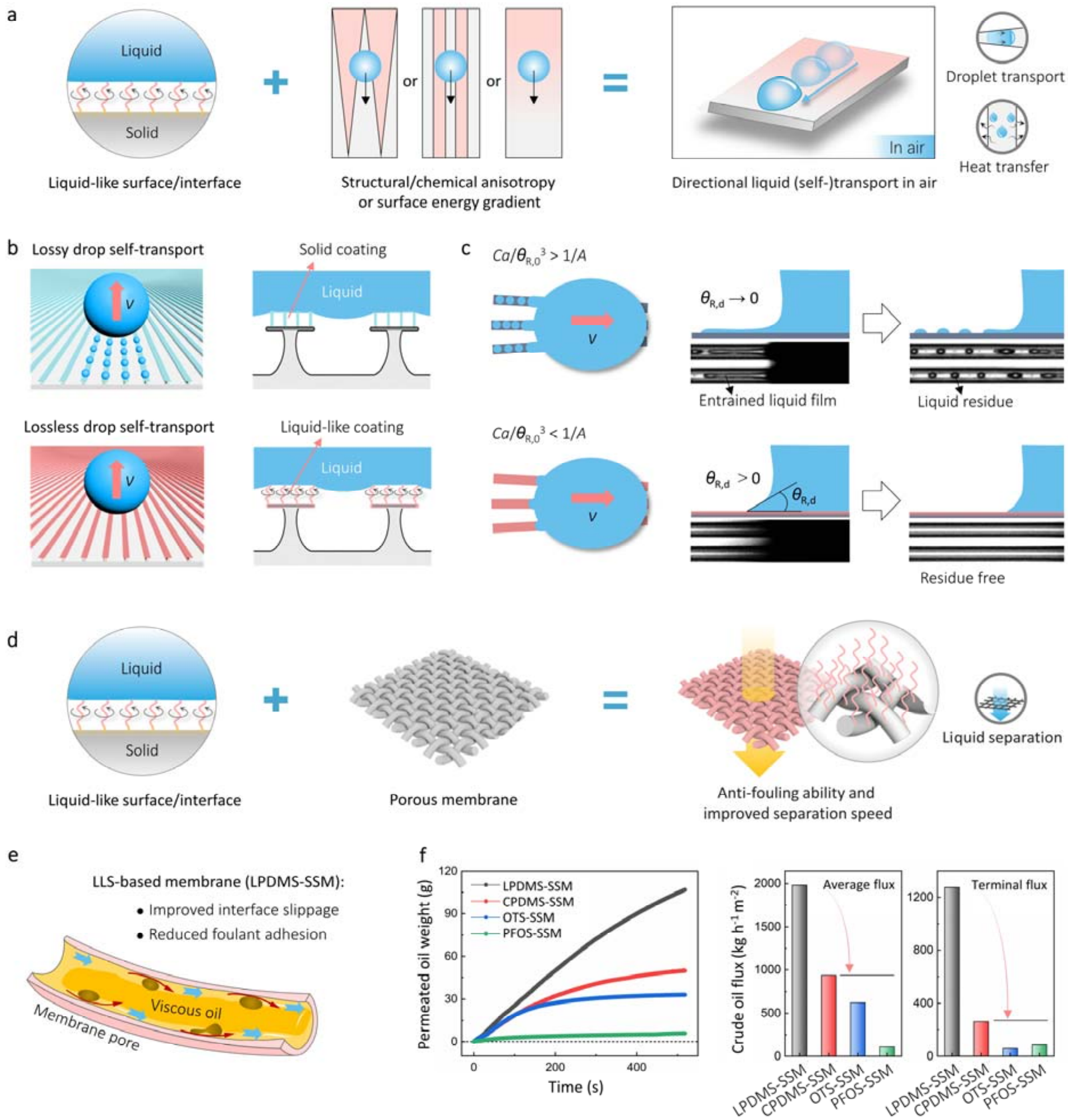

Fig. 6 Applications of patterned LLSs and LLS-based porous materials. (a) Design of the liquid-transport surfaces by combining LLSs with wetting gradient. (b) Surfaces with radially arrayed reentrant micro-orbits coated with solid PFOS layer and liquid-like PFPE layer for lossy and lossless droplet self-transport, respectively. (c) Formation mechanism of liquid residue and criterion for lossless transport. (d) Design of the LLS-based porous materials by combining liquid-like nature with porous membrane or sponge. (e) Schematic illustrating the grafted-liquid lubrication strategy for reduced foulant adhesion and promoted liquid slippage. (f) High performances of LPDMS-SSM compared with that of other solid membranes when used for separating viscous crude oil/water mixture. Panels (b) and (c) are adapted with permission from ref.[87], Wiley-VCH. Panels (e) and (f) are adapted with permission from ref.[147], Elsevier.

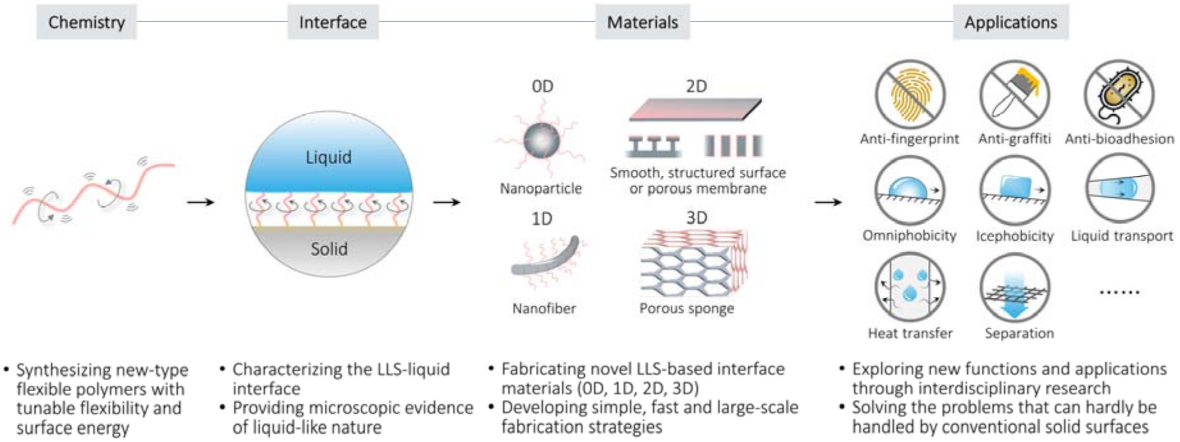

Fig. 7 Perspective on future developments and remaining challenges.

Short summary

Liquid-like surfaces (LLSs), as an emerging omniphobic system, are promising to address the challenges in minimizing interfacial adhesion towards liquids and various matters, thus enabling unprecedented functionalities that are inaccessible for conventional solid surfaces.